As originally published in the SMTA Proceedings.

SOLDER-JOINT RELIABILITY OF 0.8MM BGA PACKAGES FOR AUTOMOTIVE APPLICATIONS

Burton Carpenter
Freescale Semiconductor, Inc.
Austin, TX, USA
Burt.Carpenter@freescale.com

Thomas Koschmieder
Cirrus Logic, Inc.
Austin, TX, USA
Thomas.Koschmieder@cirrus.com

ABSTRACT

Described is experimental work to improve solder-joint reliability (SJR) of 0.8mm pitch BGA (ball grid array) packages used in automotive under-the-hood applications. Two packages were tested: a 292 IO 17mm MAPBGA and a 512 IO 25mm TEPBGA. Testing was TCoB (temperature cycle on board) in AATS (air-to-air thermal shock) between -40°C and +125°C. The target requirement was to pass 3000 cycles before first failure.

For both packages, a three factor eight-cell full factorial DOE was run to study the impact of four variables. The 292MAPBGA experiment varied solder alloy (SAC387 vs. SnAg), die thickness and die size. Solder alloy (SAC387 vs. SnAg), die thickness and PCB (printed circuit board) pad diameter were studied in the 512TEPBGA experiment.

Analyzing each experiment separately, two-parameter Weibull curves were fit to each cell, followed by regression analyses three metrics of lifetime derived from those fits. Both experiments showed packages with SnAg spheres survived longer than those with SAC387 spheres: +921 cycles (17%) for 292MAPBGA and +547 cycles (15%) for 512TEPBGA. Die size was also significant for 292MAPBGA where the smaller die survived +634 cycles (12%) longer. This result was explained by dye-and-pry analysis, which revealed solder-joint cracking progressed most quickly in the die shadow. The other factors were not statistically significant.

The best configurations from each package surpassed the requirement of 3000 cycles in -40°C to +125°C AATS. The 292MAPBGA survived over 5400 cycles and the 512TEPBGA passed 3500 cycles.

INTRODUCTION

The automotive industry continues to drive increased SJR (solder-joint reliability) for under-the-hood applications. One aspect of SJR, TCoB (temperature cycle on board) assesses thermal fatigue resistance of solder interconnection between component and PCB (printed circuit board) during temperature excursions. In some instances, requirements on number of cycles to first failure have increased 2x over previous product generations

Additionally, reliability expectations remain the same as BGA pitch shrinks to 0.8mm. Previous generations of product and associated SJR studies were typically 1.0mm pitch or greater [1, 2, 3]. Recent investigations have begun to address 0.8mm pitch [4], including the clear improvement 0.5mm/0.5mm SRO (solder resist opening) / solder sphere diameter demonstrated over the 0.4mm/0.4mm combination for the 292MAPBGA. However, other parameters needed verification, namely the effects of solder sphere alloy and die thickness. Also, this package was used for multiple devices with different die sizes. Since the die shadow had been demonstrated to influence solder-joint cracking, it was necessary to understand what effect this had on solder-joint lifetime. Additionally, SJR data was needed on a new larger package, a 25mm 512TEPBGA.

For each package, a three factor eight-cell full factorial DOE was run to study the impact of four variables: solder alloy, die thickness, die size for the 292MAPBGA and solder alloy, die thickness, and PCB pad diameter for the 512TEPBGA. SRO and solder sphere diameter were maintained at 0.5mm throughout on both. These experiments used standard daisy-chain temperature cycle testing methodology. Assemblies were monitored in situ to detect failures as they occurred, and 2-parameter Weibull failure distributions were fit to the data. Various metrics derived from the Weibull fits were regressed against their respective DOE variables to determine which had significant impact on solder-joint lifetime, and to what degree. Crack growth was assessed using cross-section and dye-and-pry techniques on unmonitored assemblies that were removed from the chambers at fixed readpoints. Conclusions on the impact of any given parameter were determined based on the totality of electrical test and crack growth data.

EXPERIMENTAL

Design and Assembly

Attributes of the packages examined experimentally are summarized in Table 1. Those highlighted in yellow were varied in the DOEs. These packages were daisy-chain test vehicles with pairs of solder-joints electrically connected as illustrated in Figure 1. A complete circuit was created by connecting pairs on the PCB side that were skipped on the package. All solder-joints in the 512TEPBGA were monitored as one "net". A failure on any solder-joint meant the remaining solder-joints could no longer be electrically monitored. The 292MAPBGA corner solder-joints were monitored independently of the other joints. In other words there were 2 nets per package.

Except where parameters were intentionally varied, the daisy-chain packages were mechanically similar to the final products: same die size, area and thickness. Similarly, the same material sets were used: mold compound, die attach, substrate materials and assembly factory.

The PCB and assembly details are in Table 2. Assembly of daisy-chain parts to boards followed industry norms. Solder paste printed to boards used the alloy Sn3.8%Ag0.7%Cu (SAC387) and a no-clean flux system. Placement of parts to boards used a dual eyepiece placement machine for aligning parts to solder-paste print. Finally, boards were run through a 10-zone reflow furnace with a peak temperature between 235°C and 245°C.

Table 1. Package details. DOE variables in yellow.

Parameter	292MAPBGA	512TEPBGA
Body Size	17mm x 17mm	25mm x 25mm
Mold Size	17mm x 17mm	22.5mm x 22.5mm
Mold Thickness	0.8mm	1.15mm
Mold Material	Epoxy Mold Compound α_1=9ppm/°C E=26GPa Tg=125°C (TMA)	
Substrate Thickness	0.38mm 4 layer	0.56mm 4 layer
Substrate Material	Epoxy Laminate α_1=16ppm/°C E=19GPa Tg=180°C (TMA)	
Die Size	1) 7.1mm x 7.6mm 2) 8.7mm x 9.5mm	8.6mm x 9.4mm
Die Thickness	1) 11 mil (279um) 2) 7 mil (178um)	
BGA Pitch	0.8mm	0.8mm
Package Pad	0.5mm SMD	
Pad Finish	Electroplated Ni/Au	
Sphere Diameter	0.5mm	
Sphere Alloy	1) SAC387 (Sn 3.8Ag 0.7Cu) 2) SnAg (Sn 3.5Ag)	

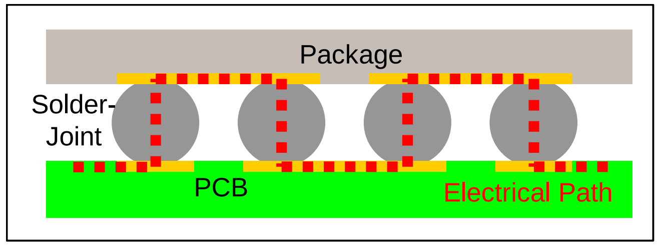

Figure 1. A daisy-chain connection representation between package substrate bottom metal and printed circuit board top metal. The red dashed line illustrates the electrical path.

Table 2. PCB and SMT assembly details. DOE variables highlighted in yellow.

Parameter	292MAPBGA	512TEPBGA
PCB Thickness:	1.60mm, 4 layer	
PCB Material	Epoxy Laminate α_1=16ppm/°C E=20GPa Tg=160°C (TMA)	
PCB Pad	0.5mm NSMD	1) 0.5mm 2) 0.4mm
Stencil Aperture Diameter	Match PCB Pad diameter	Match PCB Pad diameter
Stencil Thickness	0.100mm	
Stencil Finish	Laser cut openings with electropolish and Ni coating	
Pad Finish	OSP	
Paste	SAC387 (Sn 3.8Ag 0.7Cu)	

Typical cross-sections of components mounted on boards are shown in Figures 2 and 3 for 292MAPBGA and 512TEPBGA respectively. Key differences were package substrate thickness, mold thickness and mold cap extent. The 292MAPBGA mold cap extended across all solder-joint rows, while the 512TEPBGA mold cap extended only to the second-to-last perimeter row.

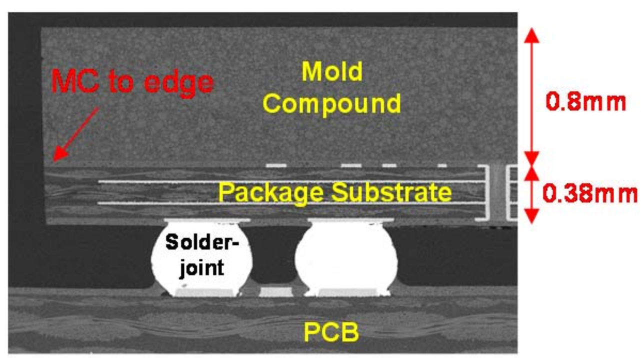

Figure 2. Typical 292MAPBGA cross-section.

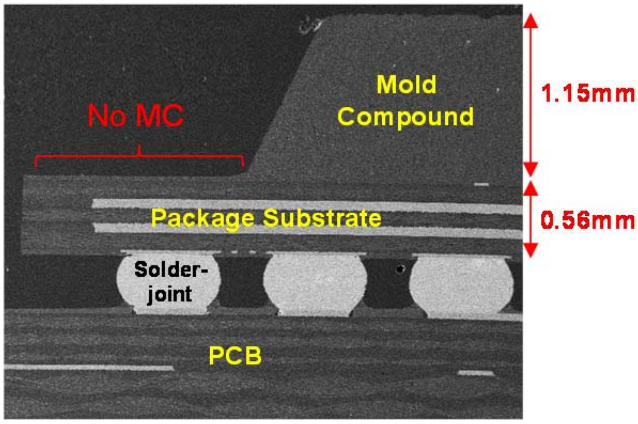

Figure 3. Typical 512TEPBGA cross-section.

Cycling, Electrical Testing and Data Analysis
Assemblies were tested in an Air-to-Air Thermal Shock (AATS) dual chamber system whereby one chamber remained hot (125°C) and the other remained cold (-40°C). An elevator system moved test boards between these chambers within about 10 seconds.

Both chamber dwell times were set at 30 minutes totaling 1 cycle/hour. Typically ~5 minutes was required to reach equilibrium, yielding ~25 min dwells. Figure 4 displays a typical temperature profile obtained by placing thermocouples in the assembly solder-joints.

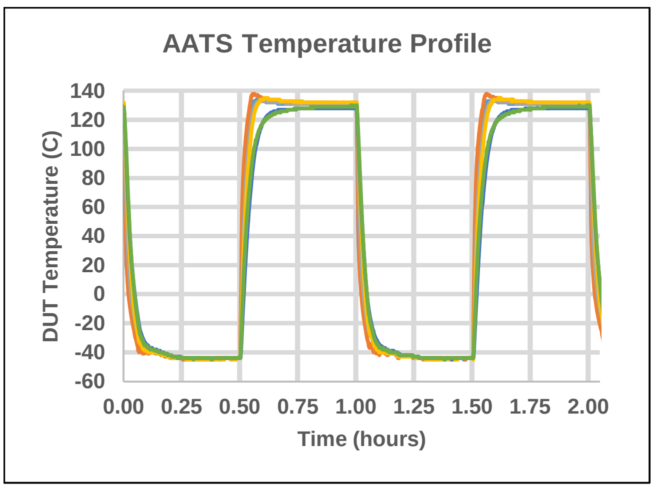

Figure 4. AATS temperature profile.

Assemblies were monitored in-situ during cycling using a 1.2mA current through each net. An event detector logged a failure when a net resistance exceeded 300 ohms. Failures were defined per IPC-9701 [5]. Generally daisy-chain resistances were few ohms at the beginning of an experiment.

Net resistance did not immediately change measurably during early stages of solder-joint crack growth, but climbed quickly as the crack approached 100%. Therefore a net failure was logged when any one of the solder-joints in that net had a crack near 100%.

For each test cell, cycling continued until at least 50% of the samples failed, after which the data were fit to a 2-paramter Weibull distribution using MLE (maximum likelihood estimate). Three metrics of solder-joint lifetime were extracted from each distribution: (1) characteristic life (Eta), (2) extrapolated number of cycles for a 1% failure rate, and (3) first failure. Each of these metrics were linearly regressed versus the DOE factors for both packages.

Crack Propagation Analysis
Two methods were used to examine crack propagation in the solder-joints during cycling: dye-and-pry and cross-section.

Dye-and-pry was a quick and simple method to obtain an overall view of cracking quantity, degree and distribution. A dye was applied to the solder-joint array to in order to mark crack locations, followed by a forced separation of package from board. Cracks formed during cycling were stained with ink, and were distinguishable from fracture surfaces created merely as a result of the forced pry [6].

Dye-and-pry had some limitations. First, it only revealed one crack interface in each solder-joint, whichever cleaved first during pry. Sometimes a solder-joint cracked along both package and PCB sides simultaneously. Additionally, PCB pads often ripped out during peel, even when solder-joint cracking had occurred. In these incidences it was assumed the degree of cracking was low (<50%) since the solder-joint strength was greater than PCB pad adhesion.

For cross-section, standard potting, sectioning, grinding and polishing techniques were used to prepare and study solder-joint crack growth. In all cases, sections were made through the joint center line. Cross-sections provided a more definitive picture of crack propagation location in the solder-joint than dye-and-pry. Often cross-section identified multiple cracks within a joint. One caution: crack front propagation may be at any arbitrary angle to the cross-section plane, thereby distorting crack length measurements.

In both DOEs, samples were removed from the chambers at various cycle counts to study degree of crack growth, location within the solder-joint, and distribution across the array. For solder-joints examined by cross-section, degree of cracking was calculated as the percentage of visible crack length divided by apparent pad diameter (all linear). For dye-and-pry, it was the crack area (red die visible) divided by pad diameter for each pad where a crack surface was revealed. See Figure 5 as an example.

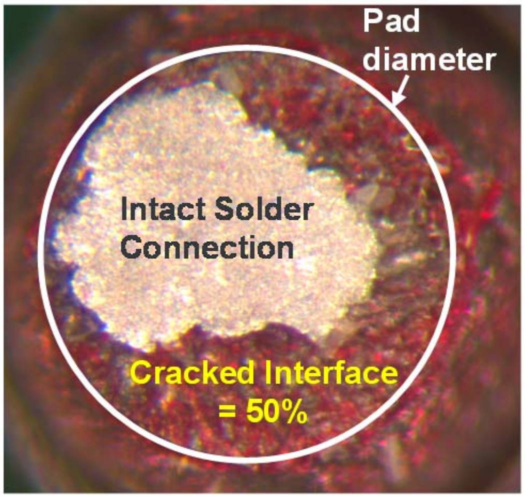

Figure 5. Example dye-and-pry image and degree of cracking calculation.

RESULTS

292MAPBGA Results

An eight-cell 2^3 full factorial DOE was conducted with the 292MAPBGA package. Die size (x-y), die thickness (z) and BGA alloy were evaluated at two levels, as summarized in Table 3. Sixteen samples were tested in each cell. Cell 3 (small, 11 mil die with SAC387 solder) was the baseline. It was hypothesized that the larger die size would decrease solder-joint lifetime, while the thinner 7 mil die and SnAg BGA alloy would both increase the lifetime.

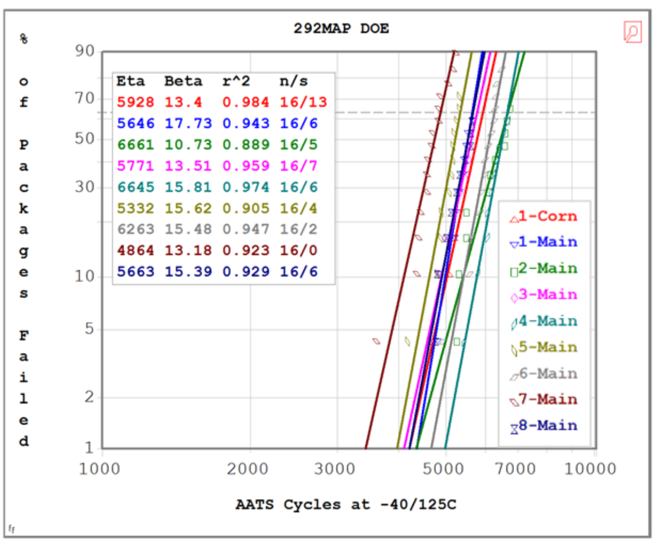

Figure 6. 292MAPBGA Weibull plots for all cells and nets. Only cell 1 had more than one corner net failures.

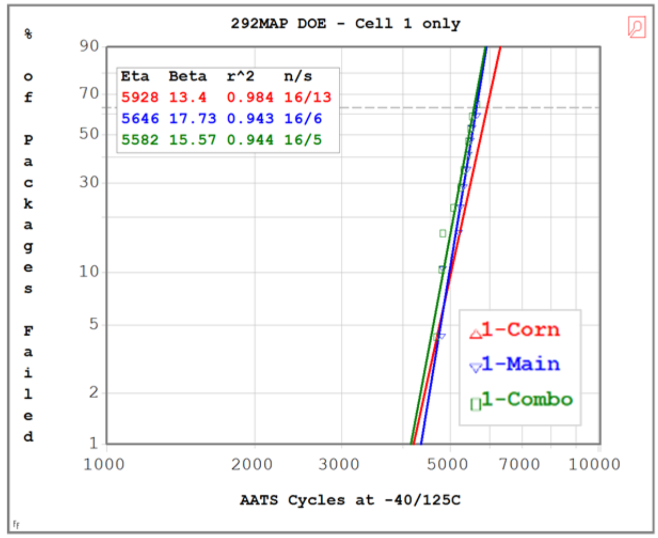

Figure 7. 292MAPBGA cell 1. The corner net, main net and combined distributions are nearly identical.

Table 4. 292MAPBGA DOE regression results. Change in solder-joint lifetime (# of cycles) for each factor.

		1st Fail	Eta	1% fail cycles
Die Size	**Small => Large**	-637	-634	*
Die Thickness	**11mil => 7mil**	*	*	*
BGA Alloy	**SAC387 => SnAg**	+814	+921	+624

* Not statistically significant

The fitted Weibull lines are plotted in Figure 6. The shape factors (Beta) ranged between 10 and 18. This indicated failures due to wear-out mechanisms rather than infant mortalities, assembly defects or secondary mechanisms. While the corner and main nets were separately monitored, only cell 1 had more than one corner net failure. A combined distribution was created for cell 1 by using each unit's first net failure. Figure 7 shows nearly identical corner net, main net, and combined distributions. Therefore the combined distribution was used in the DOE regression analysis.

Three metrics (Eta, extrapolated 1% failure cycle and first failure) were extracted from each distribution and have been summarized in Table 3. Each of these metrics was linearly regressed against the DOE factors to assess impact on solder-joint lifetimes in order to test the three hypotheses. Results are summarized in Table 4, which gives change in lifetime (# of cycles) for each factor statistically significant at the alpha=0.05 level. SnAg solder-joints lasted longer than SAC387 joints by all metrics, while the larger die decreased lifetime. Die thickness had no statistically significant impact.

After 3000 cycles, unmonitored samples from the 11mil die (cells 3, 4, 7 and 8) were removed from the chambers to examine solder-joint cracking in cross-section. As shown schematically in Figure 8, one sample from each cell was sequentially cut, polished and imaged by SEM at BGA rows A, E and G. Row A was selected to study outer perimeter and corner cracking. Rows E and G were along the die edge for the large and small die respectively.

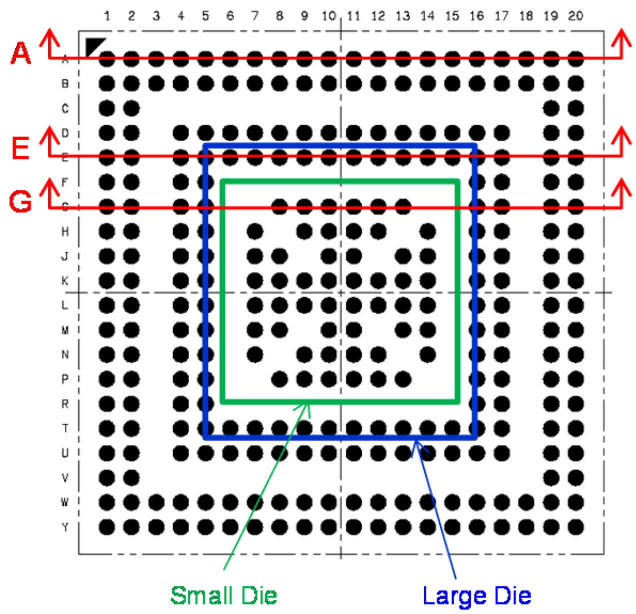

Figure 8. 292MAPBGA Cross-section locations.

Images of solder-joint E5 for each cell are shown in Figure 9. Referring back to Figure 8, this solder-joint was located under a corner of the large die, but approximately 1 mm from the small die corner. Solder-joints in proximity to a die edge (cells 7 and 8) had larger cracks. Cracks propagated along the solder to IMC (intermetallic compound) interface at the package side of the solder-joint.

By contrast, corner solder-joints in Figure 10 had a propensity for cracking on the PCB side of the solder-joint, and often had distorted shapes. This phenomena appeared isolated to corner joints, and not to other joints in close proximity. A typical example is shown in Figure 11, where the corner joint was severely damaged but the immediate neighbor had no crack propagation.

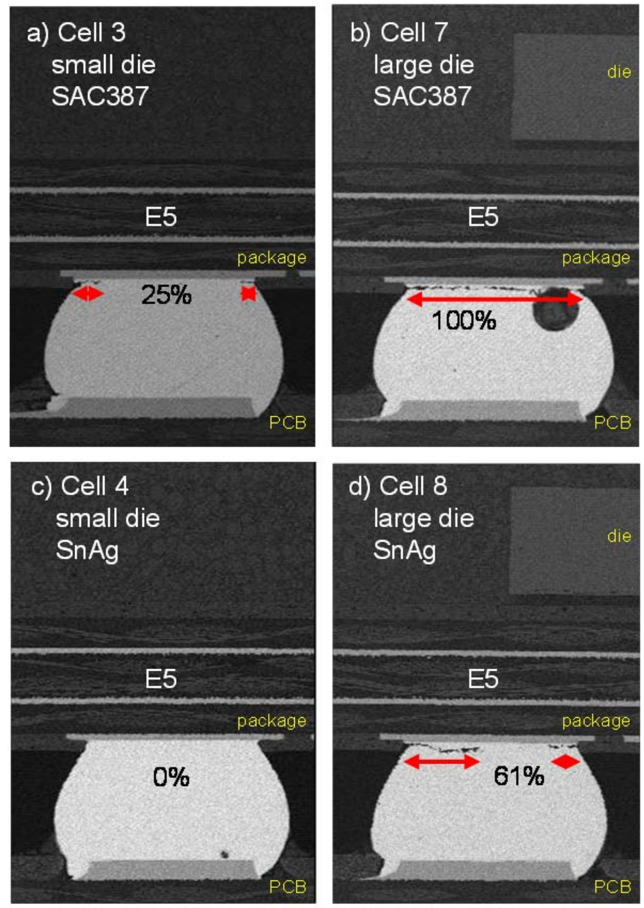

Figure 9. Cross-section of 292MAPBGA solder-joint E5 after 3000 cycles. All with 11mil thick die. Solder-joints in proximity to the die edge (cells 7 and 8) had larger cracks.

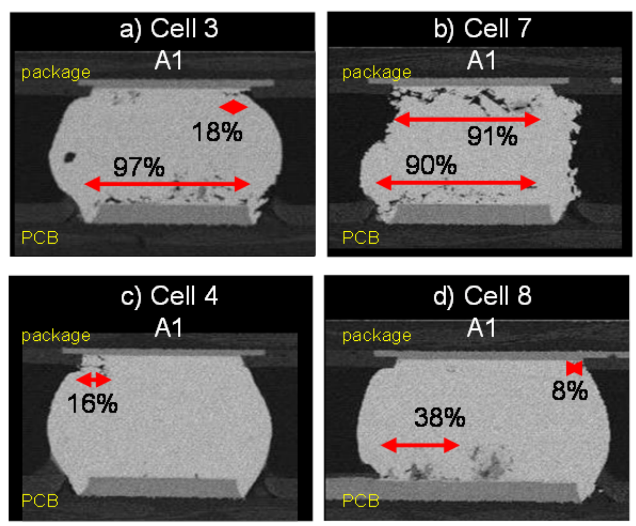

Figure 10. Cross-section of typical 292MAPBGA corner solder-joints after 3000 cycles. a) small die SAC387, b) large die SAC387, c) small die SnAg, d) large die SnAg. All with 11mil thick die. Note the propensity for cracking on the PCB side and the distorted solder-joint shapes.

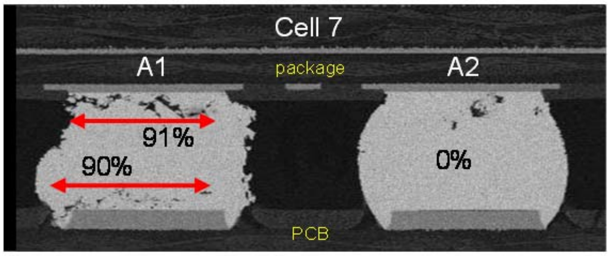

Figure 11. Cross-section of corner solder-joint A1 and neighbor A2 from 292MAPBGA cell 7 (large 11mil die with SAC387 ball) after 3000 cycles. The corner solder-joint was distorted and had significant cracking at both the package and PCB sides, but the neighbor had no appreciable damage.

For each solder-joint along the three BGA rows, degree of cracking was calculated as the percentage of visible crack length divided by apparent pad diameter. Figure 12 maps degree of cracking distributions calculated from cross-section. In general, solder-joints with cracks greater than 50% occurred near die edges or in the package comers. More advanced cracking was observed for SAC387 cells than in SnAg cells. The larger die had a slightly higher occurrence of cracking in row E than did the smaller die. Except for two corner joints, cracks greater than 50% occurred on the package side.

After 4000 cycles, unmonitored samples from the 11mil die cells (3, 4, 7 and 8) were subjected to dye-and-pry. Degree of cracking was calculated for each joint as the cracked area divided by pad area, and the distributions have been mapped in Figure 13. Joints with PCB pad rip-out are shown as green (assumed <50% crack).

In most regards, patterns emerging from the dye-and-pry distributions in Figure 13 agree with the cross-section distributions in Figure 12: cracking was most advanced near die edges, cracks propagated primarily along the solder-joint package side, and there was less cracking in SnAg samples than in SAC387 samples. However, only 2/16 corner joints cracked >50% in dye-and-pry, while 3/8 did from cross-section. This could be due to sampling variation. Another possibility was that during peel, a crack in the PCB under neighboring joints propagated under the corner joint, peeling of an entire PCB section. Figure 14 is a typical corner region image where all pads were lifted during pry.

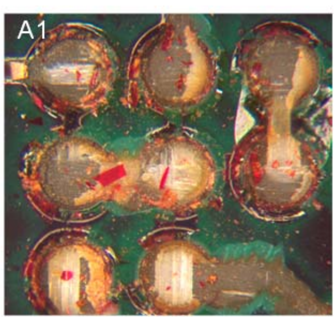

Figure 14. Example corner dye-and-pry on 292MAPBGA after 4000 cycles. This image is viewing the PCB surface.

512TEPBGA Results

An eight-cell 2^3 full factorial DOE was run for the 512TEPBGA also. Two variables were the same as before: die thickness (z) and BGA alloy. PCB pad diameter was the third. Table 5 summarizes the variables and levels. Cell 1 (11 mil die, SAC387 solder, 0.5mm PCB pad) was the baseline. Sixteen samples were tested in each cell. It was hypothesized that thinner 7 mil die and SnAg BGA alloy would both increase solder-joint lifetime, and that there would be no difference between the two PCB pad sizes.

Weibull lines fits are plotted in Figure 15. Similar to the 292MAPBGA DOE, high shape factors (Beta 8-23) indicated failures due to wear-out mechanisms.

Three metrics (Eta, extrapolated 1% failure cycle and first failure) were extracted from each distribution and have been summarized in Table 5. Each of these metrics was linearly regressed against the DOE factors to assess impact on solder-joint lifetimes in order to test the three hypotheses. Results are summarized in Table 6, which gives change in lifetime (# of cycles) for each factor statistically significant at the alpha=0.05 level. In this case, the only significant factor was solder alloy for Eta: SnAg solder-joints lasted longer than SAC387 joints.

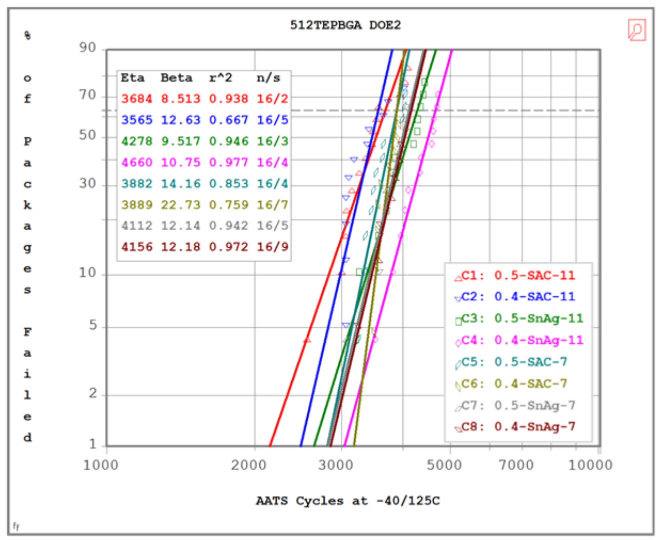

Figure 15. 512TEPBGA Weibull plots.

Table 6. 512TEPBGA DOE regression results. Change in solder-joint lifetime (# of cycles) for each factor.

		1st Fail	Eta	1% fail cycles
Die Thickness	**11mil => 7mil**	*	*	*
BGA Alloy	**SAC387 => SnAg**	*	+547	*
PCB Pad Diameter	**0.5mm => 0.4mm**	*	*	*

* Not statistically significant

Unmonitored samples from the 11mil die cells (1-4) were examined after 3164 cycles for solder-joint cracking by cross-section. As illustrated in Figure 16, one sample from each cell was sequentially cut, polished and imaged by SEM at BGA rows B, F and K. Row B was selected for cross-section analysis since it experienced more significant cracking than row A as revealed by dye-and-pry. Row K was along the die edge.

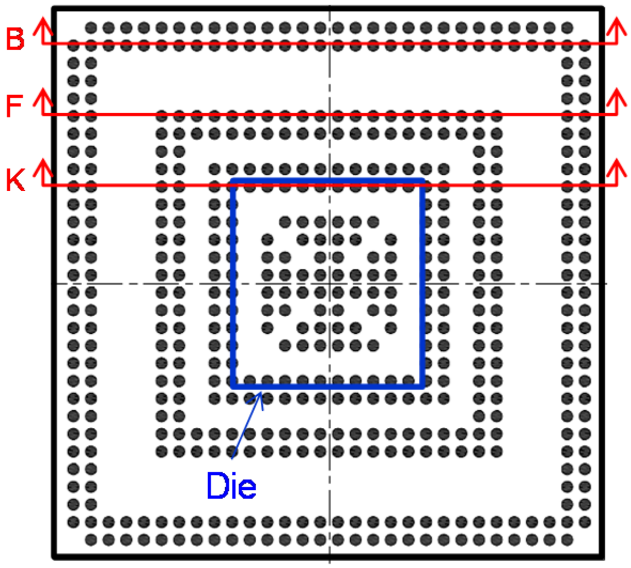

Figure 16. 512TEPBGA Cross-section locations.

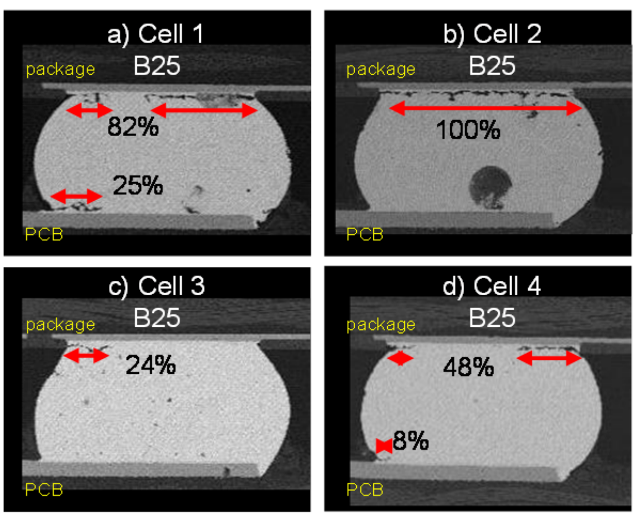

Figure 17. Cross-section of typical 512TEPBGA row B solder-joints after 3164 cycles. a) SAC387 0.5mm, PCB pad, b) SAC387 0.4mm, PCB pad, c) SnAg, 0.5mm, PCB pad, d) SnAg, 0.4mm, PCB pad,. All with 11mil thick die.

Images of solder-joint B25 for each cell are shown in Figure 17, which was chosen as a typical perimeter row sphere. Figure 18 contains images of typical joints under the die edge. In both cases, solder-joint crack propagation was primarily at the package side.

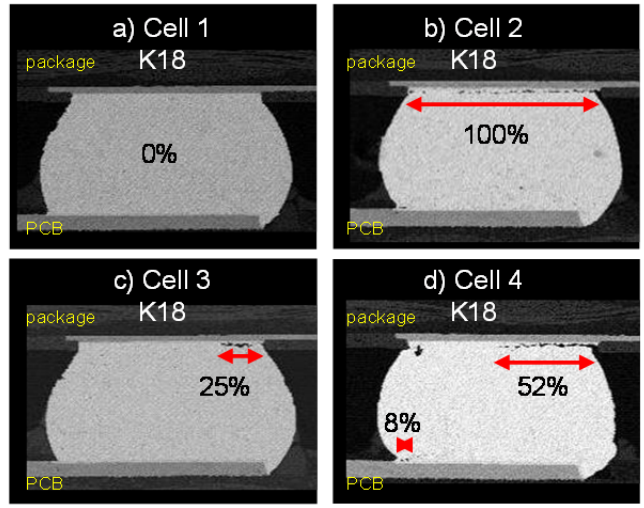

Figure 18. Cross-section of typical 512TEPBGA row K (under die edge) solder-joints after 3164 cycles. a) SAC387 0.5mm, PCB pad, b) SAC387 0.4mm, PCB pad, c) SnAg, 0.5mm, PCB pad, d) SnAg, 0.4mm, PCB pad,. All with 11mil thick die.

In the same manner as before, degree of cracking was calculated from cross-section images and the distributions mapped, as shown in Figure 19. In general, solder-joints with cracks greater than 50% occurred along row B, or the 2nd to last columns of row F (joints F2 and F29), including several with ≥90% cracking in cell 2. However, several were also observed at the die edge along row K. All cracks greater than 50% occurred on the package side. Cracking was more advanced for SAC387 spheres (cells 1 and 2) compared to SnAg spheres (cells 3 and 4), and there was a tendency for more cracking in the 0.4mm PCB pad cells (2 and 4) versus 0.5mm PCB pad cells (1 and 3).

After 4073 cycles, dye-and-pry was performed on unmonitored samples from the 11mil die cells (1-4), and degree of cracking calculated. Crack distribution maps are shown in Figure 20. The two outer perimeter rings display an interesting contrast: cracking was more advanced in the second-to-last ring. Based solely on DNP (distance to neutral point) considerations, the outermost ring should encounter the highest strain and therefore fastest crack growth. However, recall from Figure 3 that the mold cap did not extend across this outer ring, allowing stress relaxation on the outermost joints. One final observation: more cracking occurred near the package perimeter than die shadow region.

DISCUSSION

Two package systems were studied. Both were 0.8mm BGA pitch using 0.5mm diameter solder spheres on 0.5mm SRO, slated for use in automotive under-the-hood applications requiring at least 3000 cycles before failure. Differences between the 512TEPBGA and 292MAPBGA packages were the former was larger (25mm vs. 17mm), with a thicker mold cap (1.15mm vs. 0.8mm) and thicker substrate (0.56mm vs. 0.38mm), and a mold cap that did not extend to the substrate edge. In their respective DOEs, two common factors were studied: BGA solder alloy (SAC387 and SnAg) and die thickness (11mil and 7 mil).

Failure distributions from in-situ resistance monitoring during -40/125°C AATS all resulted in 2-parameter Weibull fits with high shape factors (Beta>8) indicating wear-out failures, not infant mortalities due to assembly defects or secondary mechanisms.

Since both experiments were full factorial DOEs, regression analyses were used to study which factors were statistically significant for solder-joint lifetime, and to what degree. For the following discussion, the impact of each factor has been judged based on the totality and consistency of electrical test DOE statistics and crack analysis data.

For both packages, SnAg solder sphere alloy was significantly better than SAC387 for characteristic life: +921 cycles (17%) for the 292MAPBGA and +547 cycles (15%) for the 512TEPBGA. Cross-section and dye-and-pry crack measurements corroborated this result. Degree of cracking was consistently more advanced in SAC387 samples than in SnAg ones, as seen in figures 12, 13, 19 and 20. However, crack propagation paths for non-corner joints were the same. Figures 9, 17 and 18 show this to be along the solder to IMC interface at the package side of the solder-joint.

Better performance of SnAg compared to SAC alloys has been previously reported [1, 2, 4, 7]. Eu et al. [1] reported SnAg was equal to or slightly better than SAC387 for PBGA and TBGA (tape ball grid array) packages at both 1.27mm and 1.0mm BGA pitch. Koschmieder et al. [2] found SnAg consistently better than SAC387 for 1.27mm and 1.0mm pitch PBGA. Carpenter et al. [4] observed mixed results for the 292MAPBGA, but SnAg better for a 27mm 1.0mm pitch PBGA. Meilunas et al. [7] reported longer lifetimes for SnAg than SAC387 for a large glass die in a 1.27mm pitch PBGA package.

Reasons for better performance of SnAg versus SAC alloys are still under investigation. Different IMC compositions should form during component level sphere attach. Ho et al. [8] characterized IMC growth of various Sn-Ag-Cu composition on a Ni surface. For reaction times of 10 min at 250°C, bulk solder containing little or no Cu content (≤0.2%) preferentially formed a single IMC of $(Ni_{1-x}Cu_x)_3Sn_4$ while solder with higher Cu content (≥0.6%) formed a single $(Cu_{1-x}Ni_x)_6Sn_5$ IMC. Intermediate Cu levels formed two IMC layers. At longer aging times (25hrs), the dual IMC persisted to 0.9% Cu. In the present study, SnAg should clearly form a single Ni_3Sn_4 IMC, while SAC387 should form either a single $(Cu_{1-x}Ni_x)_6Sn_5$ IMC, or perhaps a dual $(Ni_{1-x}Cu_x)_3Sn_4$ / $(Cu_{1-x}Ni_x)_6Sn_5$ structure. The dual IMC has been postulated to be more brittle than a single IMC, thus explaining better ball drop (missing solder spheres due to handling) performance of SnAg over SAC [1].

However, Cu is introduced into the SnAg solder-joint during SMT reflow. Estimated final solder-joint compositions are shown in Table 7, based solely on contributions from sphere and paste, assuming no Cu scavenging from the PCB pad. Since paste contributes less than ¼ of the final solder-joint volume, Cu content in SnAg joints remains below 0.2%, in the region of a single IMC. By contrast, Cu content remains in the dual IMC region at 0.7% for SAC387 joints. This remains under investigation, as the IMC and microstructures have not yet been fully characterized for these packages.

Table 7. Solder-joint composition after joining 0.5mm spheres with SAC387 paste, assuming no Cu scavenging from the PCB pad. Stencil thickness was 0.1mm, and stencil aperture diameter equaled the PCB pad diameter.

		Contribution by Source		Solder-joint Composition		
Sphere Alloy	**PCB Diam (mm)**	**Sphere**	**Paste**	**Sn**	**Ag**	**Cu**
SAC387	0.5	77%	23%	95.5%	3.8%	0.7%
SAC387	0.4	84%	16%	95.5%	3.8%	0.7%
SnAg	0.5	77%	23%	96.2%	3.6%	0.2%
SnAg	0.4	84%	16%	96.4%	3.5%	0.1%

It was originally hypothesized thinner die would improve solder-joint reliability due to reduced strain in the die shadow. Additionally, previous experiments and simulations suggested there may be an effect [4]. Instead, DOE regression results from the current investigation showed no significant effect in either package. This is consistent with crack measurement distributions for the 512TEPBGA (Figures 19 and 20) which indicated failures were more likely to occur in the package perimeter than in the die region. Even though failures were most likely to occur due to cracking in the die shadow for the 292MAPBGA (Figures 12 and 13), changing die thickness from 11mil (279um) to 7mil (178um) did not alter the local strain enough to cause a significant change in solder-joint lifetime.

Increasing die size significantly reduced solder-joint lifetime in the 292MAPBGA package by ~635 cycles (12%) for both characteristic life (Eta) and first failure. This correlates with distributions in Figures 12 and 13 showing cracks propagated quickest in the die shadow for this package. The larger die put more solder-joints at risk.

There was no statistically significant effect of PCB pad diameter on any solder-joint lifetime parameter in the 512TEPBGA experiment. Examination of cracking distributions in Figures 19 and 20 yield mixed results. The 0.4mm pad cells had more advanced cracking in cross-section, while the opposite occurred after dye-and-pry. This discrepancy can be attributed to sample variation. The data in total suggests that PCB pad did not play a role. Cross-section characterization of solder-joint prior to cycling showed similar average stand-off heights: 0.310mm for 0.4mm PCB pad and 0.319mm for 0.5mm PCB pad. This occurred because the stencil aperture and PCB pad diameters matched, providing additional solder volume for the larger pad. Meilunas et al. had a similar result [7]. An important consequence of this finding is that SRO:PCB pad ratio need not be strictly 1:1. PCB pad diameters can be designed at 0.4mm (50% of pitch) even when the package SRO has increased to 0.5mm, facilitating PCB routing flexibility. This will hold true whenever failures occur along the package side of the solder-joint.

These packages exhibited very different crack propagation patterns. Cracking was most severe in the die shadow and package corners for the 292MAPBGA. The 512TEPBGA by contrast demonstrated the most cracking along the second-to-last perimeter rows. Analysis can be considered for three regions: (A) package corners, (B) other non-corner perimeter, and (C) die edge/shadow. The 292MAPBGA corners differed from other perimeter joints in both failure mode (multiple cracks, including PCB side for A) and frequency (little or none for B). This unique behavior in corner spheres has been observed previously [4]. In both current and previous studies, electrical failure rates for 292MAPBGA packages with 0.5mm SRO was lower in the corners versus the rest of the array, indicating these corner cracks were not driving failures. Simulations are in progress to better understand this phenomena.

The interesting result that the 512TEPBGA second-to-last ring cracked more than the outer ring occurred because its mold cap did not extend across the outer rows allowing stress relaxation on the outermost joints. The shift from perimeter to die area cracking for the 292MAPBGA can be explained by two factors: (1) the smaller package DNP was not great enough to drive significant perimeter cracking, and (2) the 512TEPBGA thicker substrate tended to mechanically decouple the die and solder-joints.

Table 8. Cycling result comparison for similar cells. All are large 11mil thick die, 0.5mm PCB Pads.

Package	Cell	BGA Alloy	1st Fail	Eta	1% fail cycles
292MAPBGA	7	SAC387	3602	4864	3430
512TEPBGA	1	SAC387	2551	3684	2168
Ratio			1.41	1.32	1.58
292MAPBGA	8	SnAg	4762	5663	4200
512TEPBGA	3	SnAg	3209	4278	2638
Ratio			1.48	1.32	1.59

As expected, the smaller package had higher overall lifetime. Table 8 summarizes comparable SAC387 and SnAg cells from both packages. These cells all used large 11mil die size on 0.5mm PCB pad. Other parameters were the same as recorded in Tables 1 and 2. Dividing BGA array sizes (30x30 for 512TEPBGA by 20x20 for 292MAPBGA) yields a DNP ratio of 1.50. Considering the 512TEPBGA did not have corner balls, and its mold cap only extended across a 28x28 array, the DNP ratio may more properly be considered as 1.40. The ratio of lifetime metrics ranged 1.32 to 1.59, indicating an approximately linear acceleration between these two packages. Since there were various other differences between these packages (mold cap and substrate thickness), and actual strain levels were not calculated or simulated, a strict application of the Coffin-Manson equation was not warranted.

The best configuration for the 292MAPBGA was cell 4, which survived past 5400 cycles, and cell 4 for the 512TEPBGA which lasted more than 3500 cycles .

CONCLUSIONS

In situ electrical monitoring and crack propagation analysis have been completed on two 0.8mm pitch BGA packages, a 17mm 292MAPBGA and a 25mm 512TEPBGA. The primary conclusions of this study are:

1) Both packages were able to meet the required 3000 cycles to first failure in -40°C to 125°C AATS.
2) SnAg solder spheres result in better solder-joint lifetime than SAC387, +921 cycles (17%) for the 292MAPBGA and +547 cycles (15%) for the 512TEPBGA.
3) PCB pad diameter can be designed from 0.4mm to 0.5mm with similar results when using 0.5mm SRO and solder sphere on 0.8mm packages, provided failure occurs on the package side of the solder-joint.

ACKNOWLEDGEMENTS

The authors wish to recognize the support and contribution of Andrew Mawer, Paul Galles, Belinda Gonzalez, Tom Battle, Arthur Green, John Arthur, Betty Yeung, Matt Zapico, Alvin Youngblood, and Roy Arldt.

REFERENCES

[1] P.L. Eu, M. Ding, I. Ahmad, "Investigation of Sn3.5Ag and Sn3.8Ag0.7Cu Pb-free Alloys for BGA application on Ni/Au Finish" 2007 IMAPS, San Jose

[2] T. Koschmieder, J. Rayos, B. Carpenter, G. Westerman, "Comparing Electronic Component Package Materials and Substrate Vendors for Solder-Joint Reliability Improvements" 2011 SMTA International Technical Conference, Fort Worth

[3] A. Mawer and K.M. Levis, "Automotive PBGA Assembly and Board-Level Reliability with Lead-Free Versus Lead-Tin Interconnect", Journal of SMT, January 2001

[4] B. Carpenter, T. Koschmieder, B. Wilkerson, T. Hauck, J. Arthur "Design and Material Parameter Effects on BGA Solder-Joint Reliability for Automotive Applications" SMTAI 2014, Rosemont, IL

[5] "Performance test Methods and Qualification Requirements for Surface Mount Solder Attachments", IPC-9701, February 2006.

[6] T. Burnette and T. Koschmieder, "Solder joint failure analysis: Dye penetrant technique", http://electroiq.com/blog/2003/01/solder-joint-failure-analysis/

[7] M. Meilunas, A. Primavera, S. O. Dunford, "Reliability and failure analysis of lead-free solder joints", ECTC 2002

[8] C.E. Ho, R.Y. Tsai, Y.L. Line, C.R. Kao " Effect of Cu Concentration on the Reactions between Sn-Ag-Cu Solders and Ni", J. of Electronic Materials, Vol 31, No. 6, 2002

APPENDIX

Table 3. 292MAPBGA DOE electrical test results. Cell 3 was the baseline.

				Corner	Main	Overall			
Cell	**Die Size mm**	**Die Thickness mil (um)**	**BGA Alloy**	**1st Fail Corner**	**1st Fail Main**	**1st Fail**	**Beta**	**Eta**	**1% fail cycles**
1	7.14 x 7.60	7 (178)	SAC387	4680	4800	4680	15.57	5582	4155
2	7.14 x 7.60	7 (178)	SnAg	na	5247	5247	10.73	6661	4339
3	7.14 x 7.60	11 (279)	SAC387	na	4646	4646	13.51	5771	4105
4	7.14 x 7.60	11 (279)	SnAg	na	5429	5429	15.81	6645	4967
5	8.74 x 9.48	7 (178)	SAC387	na	4171	4171	15.62	5332	3972
6	8.74 x 9.48	7 (178)	SnAg	6246	4918	4918	15.48	6263	4653
7	8.74 x 9.48	11 (279)	SAC387	na	3602	3602	13.18	4864	3430
8	8.74 x 9.48	11 (279)	SnAg	na	4762	4762	15.39	5663	4200

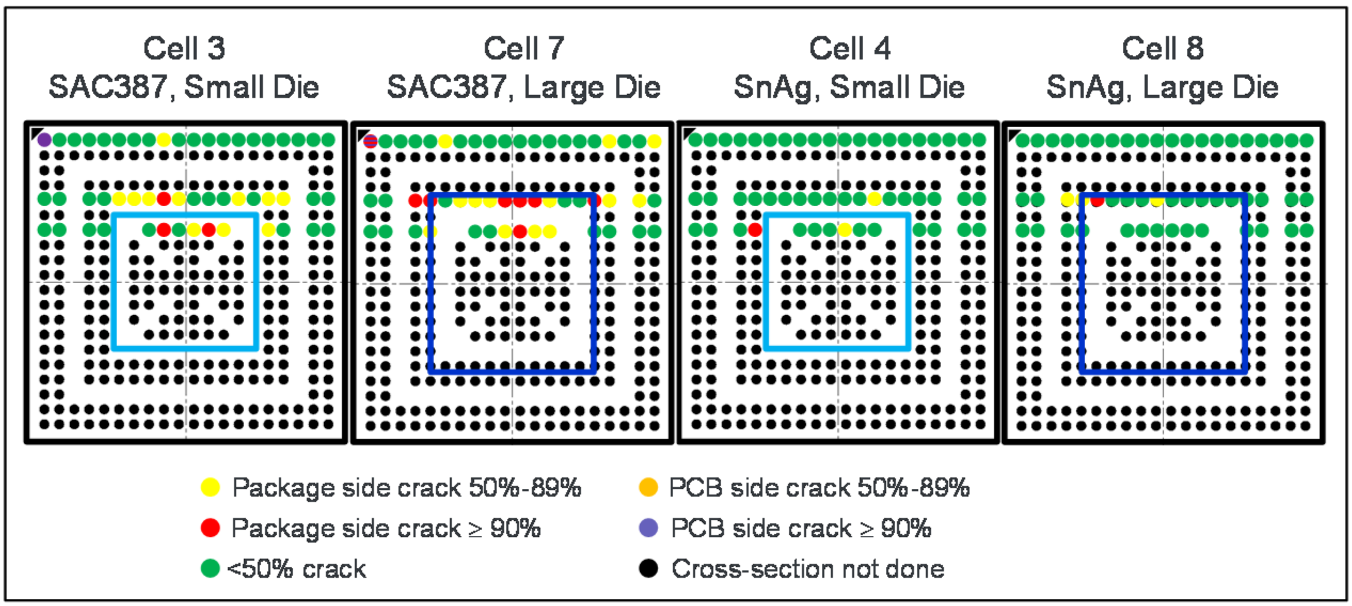

Figure 12. Degree of cracking distribution from cross-section for 292MAPBGA 11mil thick die cells after 3000 cycles.

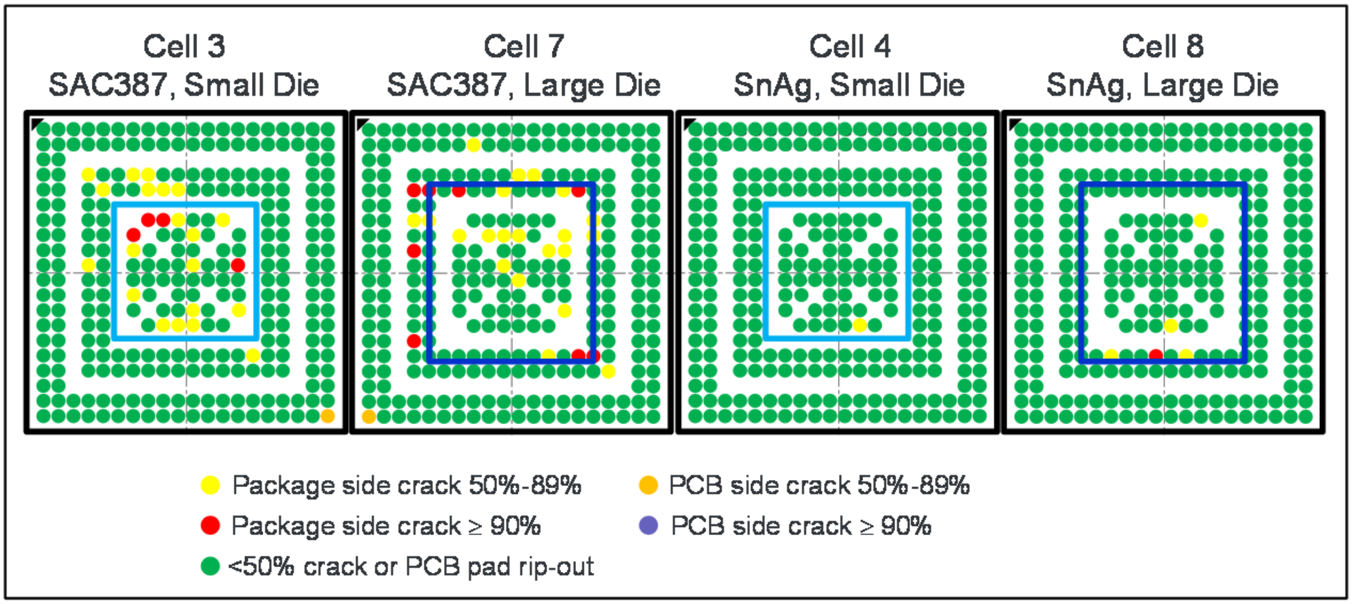

Figure 13. Degree of cracking distribution from dye-and-pry for 292MAPBGA 11mil thick die cells after 4000 cycles.

Table 5. 51TEPBGA DOE electrical test results. Cell 1 was the baseline.

Cell	Die Thickness mil (um)	BGA Alloy	PCB Pad Diameter mm	1st Fail	Beta	Eta	1% fail cycles
1	11 (279)	SAC387	0.5	2551	8.513	3684	2168
2	11 (279)	SAC387	0.4	3060	12.63	3565	2489
3	11 (279)	SnAg	0.5	3209	9.517	4278	2638
4	11 (279)	SnAg	0.4	3516	10.75	4660	3038
5	7 (178)	SAC387	0.5	3251	14.16	3882	2805
6	7 (178)	SAC387	0.4	3500	22.73	3889	3181
7	7 (178)	SnAg	0.5	3068	12.14	4112	2815
8	7 (178)	SnAg	0.4	3238	12.18	4156	2864

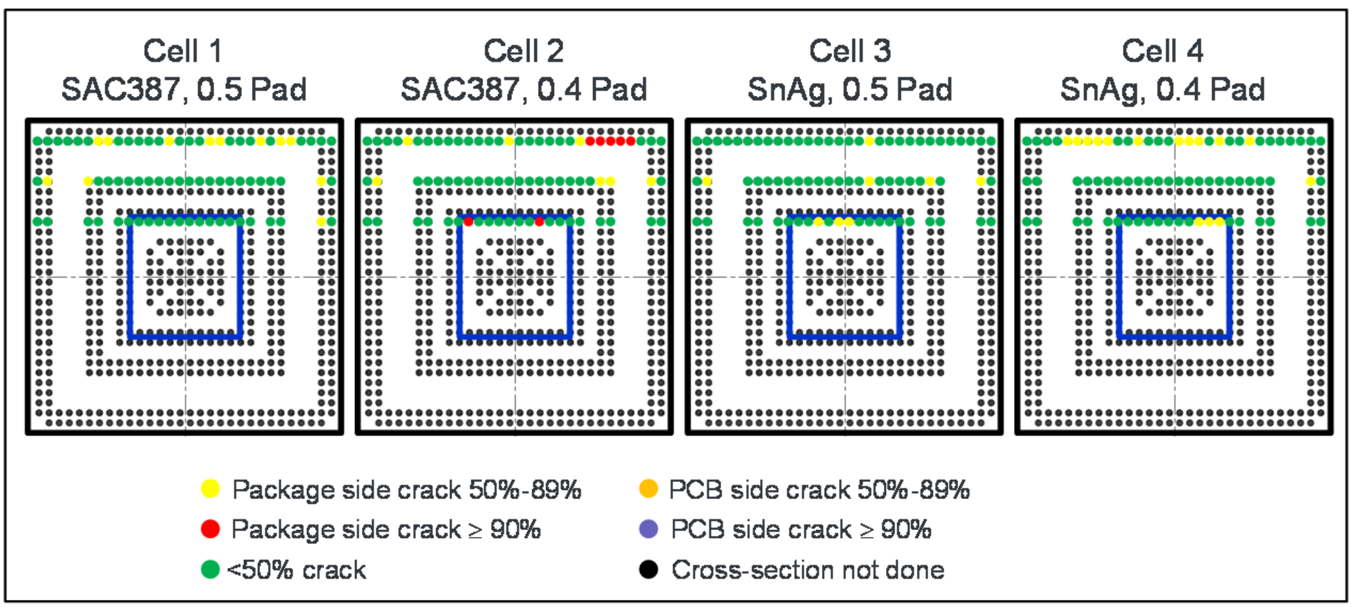

Figure 19. Degree of cracking distribution from cross-section for 512TEPBGA 11mil thick die cells after 3164 cycles.

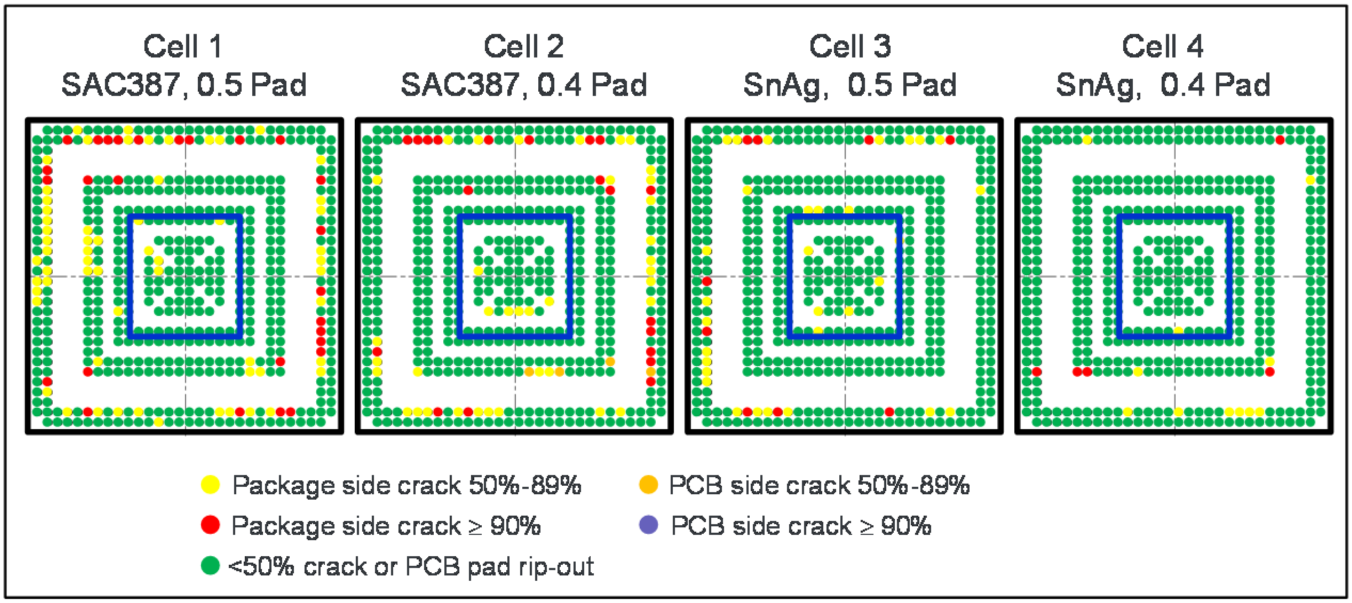

Figure 20. Degree of cracking distribution from dye-and-pry for 512TEPBGA 11mil thick die cells after 4073 cycles.